(1969).

[3]D. Emin, Phys. Rev. Letters 25, 1751 (1970).

[4]D. Emin, Phys. Rev. B 3, 1321 (1971).

[5]A. J. Bosman and H. J. van Daal, Advan. Phys. 19, 1 (1970).

[6]T. Holstein, Ann. Phys. (N.Y.) 8, 325 (1959).

[7]L. Friedman and T. Holstein, Ann. Phys. (N.Y.) 21, 494 (1963).

[8]The triple-coincidence activation energy reduces to that found by Friedman and Holstein (Ref. 7) ($\epsilon_3 = \frac{4}{3}\epsilon_2$) for the situation they consider, namely, that of the three coincident sites being mutual nearest neighbors of one another.

[9]In the limit of vanishing vibrational dispersion $\sum_{\vec{k}} q_{\vec{k}}^{\vec{b}} G_{\vec{k}}^{\vec{b},\vec{b}+\vec{h}} = A/M\omega_0^2$.

[10]In carrying out this calculation it is noted that one may replace $(G_{\vec{k}}^{\vec{b},\vec{b}+\vec{h}})^2$ by $(G_{\vec{k}}^{\vec{a},\vec{b}})^2$ in the summations over k.

[11]Recalling that $G_{\vec{h}}(T) = G_{\vec{h}}(-T)$, and that $G_{\vec{a}-\vec{b}}(0) = 1$, one may easily confirm that the conditions (i) $\Delta x_{\vec{a}-\vec{b}}(0) = 0$ and (ii) $\Delta x_{\vec{h}}(T) = 0$ are satisfied by the above expression.

[12]Explicitly, we shall see that for times short compared with $2\omega_0/\omega_1^2$ only the first and second nearest neighbors of the distorted sites are substantially involved in the relaxation process.

[13]If we do not assume the short-range linear electron-lattice interaction of Eq. (7) but a more general linear electron lattice, the constant A in Eq. (15) need only be replaced by the k-dependent coupling function $A_{\vec{k}}$.

[14]In obtaining the square-bracketed terms of Eqs. (46) and (48), we have made use of the expansion $\omega_k^{-1} = \omega_0^{-1} \sum_{n=0}^{\infty} (-1)^n [(\omega_k - \omega_0)/\omega_0]^n$ and have retained terms in these equations to order ω_b^2.

[15]Formulas (51) and (52) are obtained from Eq. (35) by inserting the relation (28) and taking the limit $T \to \infty$.

[16]Specifically, note Eqs. (80) and (89) of Ref. 4 and the discussion following Eq. (2) of Ref. 3.

[17]While it was noted in Sec. VI that the relaxation-function amplitudes $A_{\vec{b}+\vec{h}}(t)$ associated with subsequent forward and right-angle hops are not strictly equal, their very similar qualitative behavior and near equality in the short-time regime $\omega_b t \lesssim 1$ constitutes the justification of taking them to be identical in this model. In this regard, it is commented that our principal concern is for the situation characterized by most hops occurring in times less than $t_1 \sim \omega_b^{-1}$.

[18]In particular, we have compared the square of the amplitude for a double hop $1 \to 2 \to 3$ with the product of the squares of the amplitudes for the hops $1 \to 2$ and $2 \to 3$. The ratio of these expressions is given simply, in terms of the quantity E_2 defined in Eq. (3.11c) of Ref. 19, by $[\frac{1}{4} + \frac{1}{2}(E_2^* + E_2) + |E_2|^2]$, where $E_2 = 0$ at $t = 0$ and monotonically increases to the value $\frac{1}{2}$ for $t \gg \Delta t$.

[19]D. Emin, Ann. Phys. (N. Y.) 64, 336 (1971).

[20]As implied in Appendix II of Ref. 1, we may write the amplitude for a hop as the sum of contributions from successive coincidence points. The probability of a hop associated with a particular coincidence event is the sum of the square of the absolute value of the amplitude related to the above-mentioned coincidence event [the expression given by Eq. (8)] and the various cross terms involving the amplitudes for a hop at this coincidence event and at the preceding coincidences. It is the contribution of these cross terms, averaged over the appropriate occurrence-probability function, which must vanish in order to obtain formula (8). Preliminary considerations of the requisite condition for the neglect of these cross terms yields the restriction on the amount of vibrational dispersion given by the requirement (86).

[21]H. J. deWit, Philips Res. Repts. 23, 449 (1968).

[22]It is anticipated that these corrections will be reduced somewhat in a calculation for a three-dimensional model.

[23]The choice $\epsilon_2 - 5\hbar\omega_0$ was used in the earlier small-polaron papers (Refs. 1, 2, 4, 7, and 19). If one assumes that $\omega_b/\omega_0 = \omega_1^2/2\omega_0^2 \approx M_2/4M_1$ (Ref. 21) and takes M_1 and M_2 to be the atomic masses of nickel and oxygen, respectively, then one sees that the choice $\omega_b/\omega_0 = 0.07$ is appropriate to NiO.

PHYSICAL REVIEW B VOLUME 4, NUMBER 10 15 NOVEMBER 1971

Optical Response of AgCl and AgBr in the Near and Extreme Ultraviolet*

Nicholas J. Carrera† and Frederick C. Brown
Department of Physics, University of Illinois, Urbana, Illinois 61801

(Received 15 March 1971)

The extinction coefficients of AgCl and AgBr have been obtained down to liquid-helium temperature by observing the transmission of thin films in the near-uv direct exciton region (3.5–6.7 eV) and in the extreme uv (30–240 eV) using synchrotron radiation. The index of refraction was determined for both materials by a dispersion relation, and the optical constants were then constructed for AgCl in the range 3–240 eV, using all available data. Some interpretation of the exciton and band-to-band spectra is given. An estimate is made of the effective number of electrons which contribute to the absorption over a wide range of photon energies.

I. INTRODUCTION

The characteristic optical absorption of AgCl and AgBr begins in the near ultraviolet at photon energies of approximately 3 eV. Measurements on single crystals indicate that the absorption tails in this region are strongly temperature-dependent according to the so-called Urbach rule.[1,2] Detailed investigations down to liquid-helium temperatures on the pure materials[3] and also on mixed crystals[4]

confirm the indirect or phonon-assisted nature of the absorption thresholds as suggested by Seitz.[5] Subsequently, band calculations[6,7] showed that, although the uppermost filled band is formed from the *np* atomic states of the halogen ions as in the alkali halides, the valence bands have maxima in more than one direction away from the center of the Brillouin zone. This is due to strong mixing with the silver 4*d* states, whose levels lie only an eV or so below the halogen levels. The mixing is sensitive to the lattice parameter[8] and, in fact, Bauer and Spicer[9] have suggested the existence of dynamic effects in order to explain their large temperature-dependent photoemission results. The piezomodulation work of Ascarelli[10] indicates that the maximum of the valence band is at the zone boundary in the ⟨111⟩ directions, so that a longitudinal acoustic phonon must either be emitted or absorbed in an optical transition to the conduction-band minimum at Γ_1.

The indirect absorption of the silver halides extends for nearly 2 eV above threshold and rises to values of the absorption coefficient somewhat in excess of $10^3\,\mathrm{cm}^{-1}$. Beginning in the range 4–5 eV, the optical response increases very rapidly as a result of direct transitions. Here, maximum absorption coefficients are 10^5–$10^6\,\mathrm{cm}^{-1}$, and the structure is similar to that observed in the alkali halides, including the halogen spin-orbit splitting. Reproducible thin film absorption measurements were reported many years ago by Okamoto[11] and by Tutihasi.[12] More recently, careful reflectivity spectra were obtained out to 20 eV for AgCl by White and Straley[13] and for AgBr by White.[14] These reflectivity measurements were made on polished crystalline samples at room temperature.

Excitons are expected to play a role in both the direct and indirect regions, and, indeed, the thin film data show strong direct exciton lines, especially at low temperature. From results on thin (20 μ) platelets of AgCl, it was suggested by Giammarinaro and co-workers[15] that the direct exciton lines previously observed are to be associated with molecular transitions rather than with transitions near the center of the zone for the crystal. Their suggestion can hardly be taken seriously, however, since tests show[16] that their samples were much too thick to properly reveal the strong direct exciton absorption in these materials. Moreover, reflectivity[13] and thin film transmission data agree fairly well in the direct exciton region. Further results are given below for well-characterized thin films at various temperatures down to that of liquid helium. The ultraviolet exciton absorption appears to be a property of the bulk crystal and is understandable within present concepts.

At sufficiently high photon energies, say above 30 eV, it becomes possible to excite electrons from very low-lying states into the conduction band. These "core" levels are narrow in energy and nearly flat throughout the Brillouin zone because the wave functions for inner-shell electrons experience little overlap with wave functions on neighboring ions. The over-all transition rate for excitation of these core levels will thus be determined primarily by the final conduction-band density of states as well as by matrix elements between initial and final states. The measurements reported below allow a detailed comparison to be made between the low- and high-energy uv spectra.

The present work was also undertaken in order to display the behavior of optical constants over an unusually wide range of quantum energy in at least one class of substance. As expected, it was found that the index of refraction approaches very close to 1.00 in the extreme uv. The results permit one to test sum rules and to ascertain the effective number of electrons which contribute at a given quantum energy. In the course of these investigations the effect of strain on the silver halide exciton line was investigated and differences were sought between the results obtained from thin film transmission and the reflection of single crystals. In many respects the silver halides appear to be model substances for testing our present understanding of optical response and band structure.

II. EXPERIMENTAL METHOD

Thin samples of somewhat different thickness were required for transmission measurements in the uv (3.5–6.7 eV) and extreme uv (30–240 eV) regions. For example, films of the order of 1000 Å could be used for the extreme uv, while only a few hundred Å thickness was required for the uv. In both cases they were prepared by vacuum evaporation onto thin transparent substrates of Formvar (polyvinyl formal resin) or Lucite. For the low-energy range, the samples were prepared in a well-trapped vacuum evaporator at a pressure of 10^{-7} Torr and then transferred under inert atmosphere to a liquid-helium cryostat.[4] In the case of the high-energy range, the samples were evaporated *in situ* at the storage ring light source as described elsewhere.[17] In some cases the quality of the films was investigated by means of electron diffraction.

The technique of preparing and supporting the substrates was similar to that described by Bachrach.[18] It can be briefly summarized as follows. Formvar or Lucite is dissolved in ethylene dichloride and a drop is placed onto the surface of deionized water. After evaporation of the solvent, the film, about 250 Å thick was lifted off and placed over a washer having a hole of diameter $\frac{3}{16}$ in. The substrate film, thus supported only on the edges, could be easily handled by means of the washer which was then clamped in a spring-loaded

cartridge. Initially, the washers were made of crystalline AgCl or AgBr to minimize strain due to differential contraction upon cooling. This made little difference, however, unlike the thallous halides.[18] Lucite and Formvar gave similar results, but the latter was preferred because of greater transmission, strength, and resistance to radiation damage in the high-energy region.

The sample material, high-purity silver halide crystals, was contained either in quartz or in platinum crucibles. Both AgCl and AgBr readily evaporate just above their melting points without excessive dissociation. In the present case the deposition rate was carefully controlled and held to about 10 Å/min. The rate of deposition and film thickness were determined by a 5-MHz quartz-crystal thickness monitor calibrated by the Tolansky interference technique. Final thickness ranged from 150–2000 Å. Although the uncertainty of measurement of the thickest films was only about 5%, the thinner samples had an uncertainty in thickness of 10–15%. This latter uncertainty carried over to the extinction coefficients of AgCl in the uv exciton region. Absolute values of the maximum extinction for AgBr were uncertain by perhaps as much as 25%.

In the uv range, a Cary model 14R spectrophotometer was used to determine the wavelength dependence of the optical density D given by

$$D = \log_{10}(I_0/I) \ , \tag{1}$$

where I_0 is the incident intensity and I the transmitted intensity. When interference effects can be neglected, it is easy to show that the ratio I/I_0 is given by

$$\frac{I}{I_0} = \frac{(1-R)^2 e^{-\alpha t}}{1-R^2 e^{-2\alpha t}} \ , \tag{2}$$

where R is the reflectivity, t is the sample thickness in cm, and α is the absorption coefficient in cm^{-1}. Equation (2) applies to a sample bounded on both sides by vacuum, but is also a good approximation for the film-substrate combination used in the present work as discussed by Bachrach.[18] Furthermore, the error introduced in the uv by setting $R = 0$ has been estimated to be less than 10%. By measuring the optical densities D_1 and D_2 for two sample thickness t_1 and t_2, uncertainty due to reflection loss can be further minimized and account can be taken of substrate absorption. In this case the absorption coefficient α (cm^{-1}) can be determined from the relation

$$D_2 - D_1 = \alpha(t_2 - t_1)/2.303 \ . \tag{3}$$

If one wishes to specify the response of the sample by the optical constants n and κ as they enter into a complex index $\tilde{n} = n - i\kappa$, the following simple relation between α and κ can be used:

$$\kappa = \lambda\alpha/4\pi = (\hbar c/2E)\,\alpha \ , \tag{4}$$

where E is the photon energy.

The spectrophotometer scans were made at room temperature and with liquid nitrogen and liquid helium in the cryostat. Temperatures were measured with thermocouples and with a calibrated germanium thermometer. The cryostat was well shielded, and in the liquid-helium runs it was estimated that the sample temperatures were close to that of the cold finger connecting to the cryogenic fluid. Thus, for liquid helium the sample temperature was in the range 5–10 °K; for liquid nitrogen in the range 77–80 °K. Little rise in temperature and no degradation of the films was observed upon exposure to uv light.

The extreme uv measurements were made at the University of Wisconsin physical science laboratory using synchrotron radiation from the 240-MeV electron storage ring. The radiation obtained from this type of source is intense, highly collimated, and continuous in energy, making it ideally suited for transmission measurements in the high-energy range above 20 eV. Since details of the use of an electron storage ring for spectroscopy have been presented elsewhere,[17,19] only a very brief discussion will be given here.

In the UWPSL machine, electrons from a 50-MeV accelerator are captured into the storage ring, accelerated slowly to 240 MeV and held in a stable orbit for decay times which can be several hours. During this time, while passing through the bending magnets, they radiate a continuum which extends from the infrared out to 50 Å or less in the soft x-ray region. The energy lost by radiation is continuously supplied by a rf source at 32 MHz (the frequency of revolution of the electrons in stable orbit). The current of circulating high-energy electrons is typically 5–10 mA, and the data is taken as this beam slowly decays.

As shown in Fig. 1, light from the storage ring passes through the sample region and is focused onto the entrance slit of a 86° grazing incidence spectrometer. This instrument (Hilger-Watts E580) was modified and adjusted for use with the synchrotron source so that with a 576-line/mm grating the spectral bandpass was better than 0.1 A. A Bendix extended-cone Channeltron was employed to count individual photons. The Channeltron counting rate, a signal from an encoder on the spectrometer wavelength drum, and a digitized signal proportional to the incident beam intensity were recorded by teletype on punched paper tape during continuous wavelength scans. The scanning rate could be reduced in regions containing structure, and repeated scans could be combined during computer handling of the data.

All of the components in the optical path of Fig.

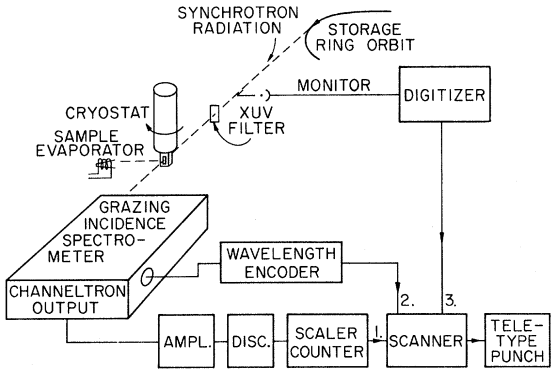

FIG. 1. Apparatus for measuring the transmission of thin films in the extreme uv using synchrotron radiation.

1 were in a common vacuum. The tail of the rotatable helium cryostat actually had provision for mounting up to four substrates. In most cases these were Formvar substrates; however, for measurements near photon energies of 200 eV, very thin gold substrates were used. The extreme uv transmission of a substrate could be measured and then the cryostat rotated so that the substrate faced an evaporator gun. In this way, the silver halide could be deposited *in situ* under high vacuum with cold baffles surrounding the sample. Again, deposition rate and thickness were monitored by a quartz oscillator.

The extreme uv absorption coefficients were obtained from the observations with the help of Eqs. (1)–(3). The approximations mentioned in connection with these relations were closely satisfied because of very small reflectivity R in the extreme uv. In fact, at the higher energies, when the substrate density was known from a prior measurement, it was a good approximation to use $\alpha t = 2.303D$ for a sample of known thickness t and measured optical density D. It was, however, necessary to be careful about the presence of stray light. Aluminum, gold, or polypropylene filters could be rotated into the incident beam for the purpose of suppressing stray light in the various ranges of wavelength. In some cases, an estimate of the stray light was made by varying the storage ring energy. Corrections to the data could then be made.

Using Eq. (4) it was a simple matter to obtain the extinction coefficient κ from the absorption coefficient α. On the other hand, the index of refraction at frequency ω_p had to be determined by means of a Kramers-Krong relation[20] as follows:

$$n(\omega_p) = 1 + \frac{2}{\pi} \mathcal{P} \int_0^\infty \frac{\omega \kappa(\omega)}{\omega^2 - \omega_p^2} \, d\omega \,, \tag{5}$$

where $\mathcal{P}$ indicates the principal part of the integral. Numerical methods can be used to evaluate the integral in Eq. (5), but the convergence in ω is slow (of the order of $1/\omega$ for large ω). More rapid convergence can be obtained by referring the index at frequency ω_p to a known index $n(\omega_0)$ at frequency ω_0. A subtracted dispersion relation can easily be derived from Eq. (5) with the following result:

$$n(\omega_p) - n(\omega_0) = \frac{2}{\pi} (\omega_p^2 - \omega_0^2) \mathcal{P} \int_0^\infty \frac{\omega \kappa(\omega) d\omega}{(\omega^2 - \omega_0^2)(\omega^2 - \omega_p^2)} . \tag{6}$$

Because this relation converges more rapidly ($1/\omega^3$ at large ω), the extinction coefficient need be known only over a restricted range of energy. Various cutoff or extrapolation procedures can be tried over the range of known κ. Both Eqs. (5) and (6) and different methods of numerical integration were employed in order to obtain the index of refraction in the present work.

The real and imaginary parts of the dielectric response function $\tilde{\epsilon} = \epsilon_1 - i\epsilon_2$ were obtained from n and κ by means of the usual relations

$$\epsilon_1 = n^2 - \kappa^2 \,, \tag{7}$$

$$\epsilon_2 = 2n\kappa. \tag{8}$$

When $\epsilon_2(E)$ is known as a function of photon energy $E = \hbar\omega$, it is possible to evaluate $N_{\text{eff}}(E_0)$, the effective number of electrons which contribute to optical absorption over a range of energy up to E_0. This is especially useful at and above the thresholds corresponding to excitation of the various core electrons. We use a modification of an expression given by Philipp and Ehrenreich,[21]

$$N_{\text{eff}}(E_0) = \frac{2m}{e^2\hbar^2} \frac{A}{L\rho} \int_0^{E_0} E \, \epsilon_2(E) \, dE \,, \tag{9}$$

where A is the atomic weight, L is Avogadro's number, and ρ is the density. Results are given in Sec. III from data taken in both the uv and extreme uv energy ranges.

III. EXPERIMENTAL RESULTS

Results for the uv region of the spectrum will be presented first. Figures 2 and 3 show the measured absorption coefficients in the vicinity of the fundamental edge for AgCl and AgBr at liquid-helium temperature. Such curves were taken with a very high spectral resolution of 0.002 eV or better. These measured curves agree qualitatively with the lowest temperature results of Okamoto[11] and clearly show the strong excitonic absorption overlying the fundamental edge. These data were obtained on well-characterized films, and the observations showed a high degree of reproducibility. The peak position and structure for AgBr could be reproduced for different films within ±0.002 eV. A very small variation (±0.05 eV) in the first ex-

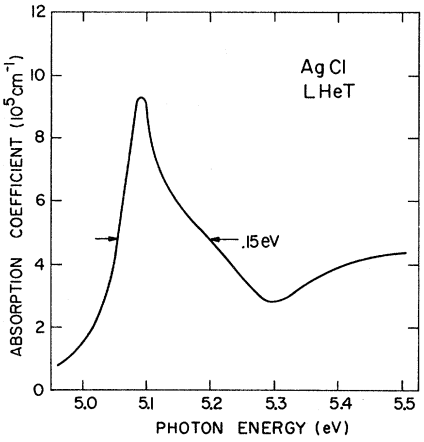

FIG. 2. Direct exciton peak for AgCl at liquid-helium temperature obtained by means of uv transmission measurements on thin films. A spectral bandwidth of about 0.002 eV was employed.

citon peak position for AgCl was observed, but this might be due to residual strain effects. It is inconceivable that these peaks are due to excitation states of isolated molecules, as recently suggested.[15]

Exciton lines usually show a strong narrowing with decreasing temperature. This is clearly seen in the extinction coefficient data taken at three different temperatures for AgCl (Fig. 4) and for AgBr (Fig 5). The indices of refraction shown in these figures were obtained by means of Eq. (6), referring to a value of $n(\omega) = 2.071$ for AgCl and 2.253 for AgBr, both measured at $E = 2.104$ eV in the

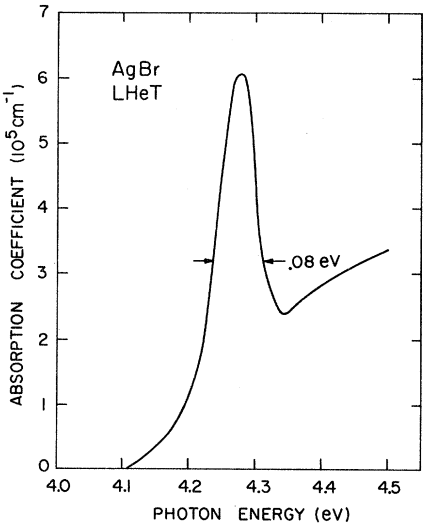

FIG. 3. Direct exciton peak for AgBr at liquid-helium temperature obtained by means of uv transmission measurements on thin films. A spectral bandwidth of about 0.002 eV was employed.

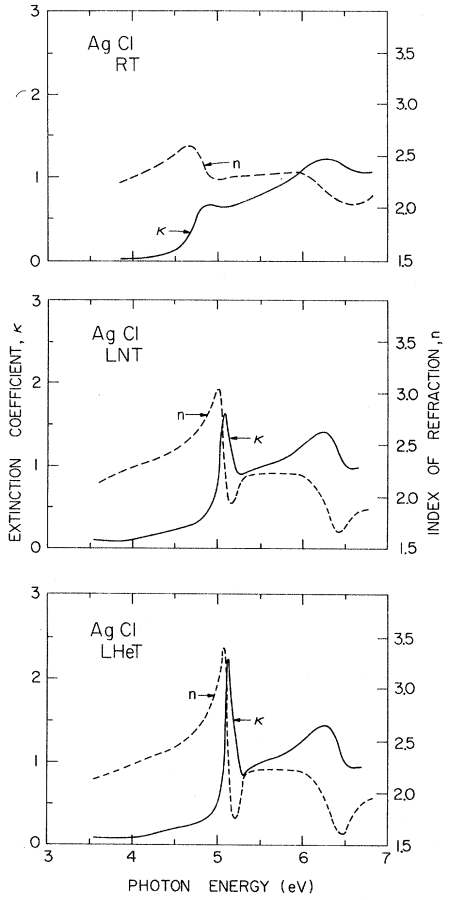

FIG. 4. Optical constants n and κ in the uv for AgCl at room, liquid-nitrogen, and liquid-helium temperatures.

visible part of the spectrum.[22] Besides the dramatic narrowing of the exciton structure with decreasing temperature, it can be seen that there is a shift to higher energy. This is similar to the behavior of the indirect edge and is largely due to an increase of the band gap with decreasing temperature.[3,4]

The absorption coefficients in the extreme uv for AgCl and AgBr are shown in Fig. 6. There was remarkably little difference in these high-energy spectra upon cooling to low temperature. The absorption for silver metal is also shown in Fig. 6 as determined in the work of Haensel *et al.*[23]

The room-temperature values of uv extinction for AgCl, shown in Fig. 4, extend out to about 7 eV. By means of $\kappa = \lambda\alpha/4\pi$ [Eq. (4)] it is easy to convert the absorption coefficients of Fig. 6 to extinction, and these data then cover the range 30–240 eV. Fortunately, there exist reliable published data for AgCl in the range 6.7–30 eV. Using these data of White and Straley[13] in the intermediate range, it is possible to construct the extinction coefficient κ for AgCl over the entire

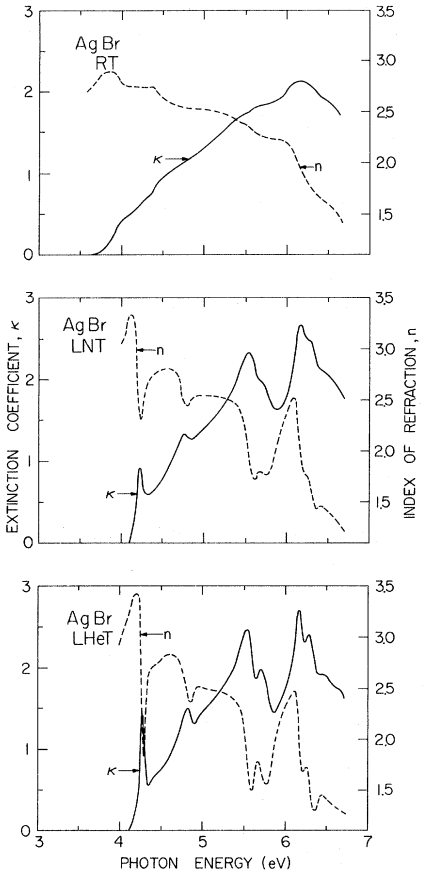

FIG. 5. Optical constants n and κ in the uv for AgBr at room, liquid-nitrogen, and liquid-helium temperatures.

range 3.5–240 eV.[24] The results are shown in Fig. 7.

The index n can now be evaluated by a Kramers-Kronig analysis over the entire range. When computing n in the extreme uv, particular attention must be given to the contributions in the low-energy uv because of the large extinction in that region. The analysis was carried out using both Eqs. (5) and (6) with essentially identical results. Figure 7 contains the calculated curve for n along with extinction coefficient κ. Notice how the values of n closely approach 1.0 in the high-energy range above 100 eV. This is, of course, because of diminishing contribution from κ toward high energy. Below 25 eV, our calculated values of index n agree well (differing by less than 10%) with the results of White, who calculated n from his reflectivity data using a dispersion relation relating phase shift and reflectivity.

It would also be possible to construct n and κ curves from 2.5 to 240 eV for AgBr, except that good data in the intermediate range out to 25 eV have not yet been published.[14] The AgBr data of Koester and Givens,[25] together with a smooth interpolation from 13 to 30 eV, is not satisfactory.

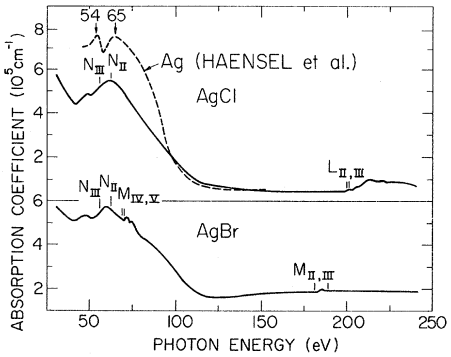

FIG. 6. Solid lines show the measured absorption coefficients for AgCl and AgBr in the extreme uv from 30 to 240 eV. Dotted line in the upper part of the figure shows the absorption of silver metal from Haensel *et al.* (Ref. 23).

The real and imaginary parts of the dielectric response function were computed for AgCl over the entire range using Eqs. (7) and (8). Results are shown in Fig. 8. A log-log scale allows us to cover the entire range of ϵ_2. The $L_{II,III}$ threshold, due to the Cl^-2p^6 electrons, can be clearly seen at 200 eV. Detail in the absorption coefficient at, and just beyond, this $L_{II,III}$ edge is shown in Fig. 9, where the numbers label reproducible structural features which are listed in Table I.

Finally, we plot the effective number of electrons $N_{eff}(E_0)$ as a function of E_0 for AgCl in Fig. 10. For this purpose the values of ϵ_2 plotted in Fig. 8 were inserted into Eq. (9) and numerical integration was carried out. The possible number of electrons which can contribute are shown in Fig. 10 at energies corresponding to the core thresholds given by Bearden and Burr.[26] At 50 eV, just below the energy at which transitions from the silver $4p$ states can occur, there are a possible 18 electrons

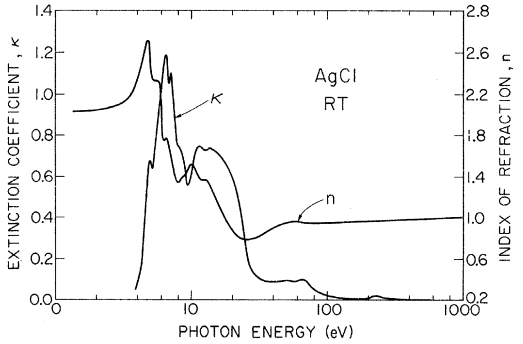

FIG. 7. Optical constants n and κ over the extended range 3.5–240 eV for AgCl at room temperature. Constructed from the present data plus the results of White and Straley (Ref. 13).

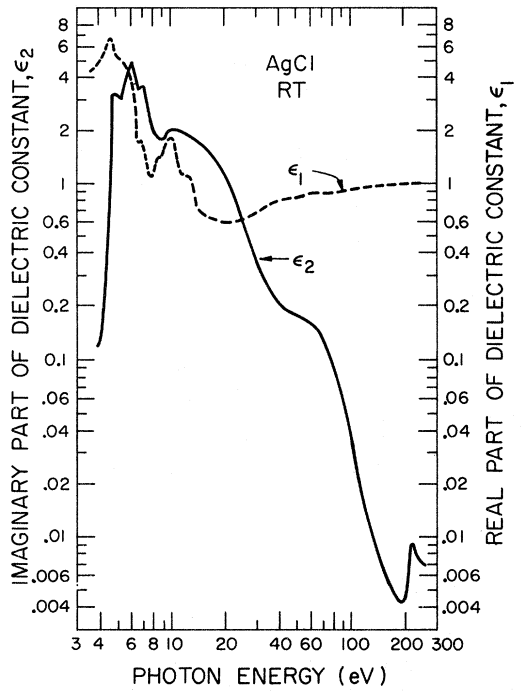

FIG. 8. Real and imaginary parts of the dielectric response function for AgCl at room temperature over the extended range 3.5–240 eV.

which can contribute to absorption. This compares with N_{eff} at 50 eV equal to about 14. At 200 eV, just *below* the $Cl^- L_{II,III}$ edge, 26 electrons can contribute, whereas N_{eff} at 200 eV is equal to 24. Note that N_{eff} rises more steeply as E_0 passes through regions of strong absorption. For example, at 50–60 eV the silver $N_{II,III}$ or $4p$ threshold occurs.

A diagram which shows schematically the various valence and core energy levels expected for silver, chlorine, and bromine is given in Fig. 11. The

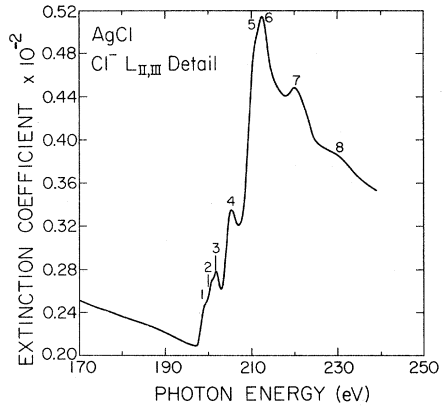

FIG. 9. $L_{II,III}$ extinction of AgCl on an expanded scale. Numbers refer to structural features listed in Table I.

TABLE I. Spectral features observed at and just beyond the chlorine $L_{II,III}$ edge of AgCl shown in Fig. 9.

Feature No.	E (eV)	$E-197.6$ (eV)	Tentative assignment
Threshold	197.6	0.0	Γ_1
1	199.0	1.4	Δ_1-X_1
2	200.8	3.2	spin orbit of 1
3	201.7	4.1	L_2,
4	205.4	7.8	X_3
5	210.5	12.9	
6	212.2	14.6	
7	220	22.4	
8	230	32.4	

numbers shown in this diagram are the energies in eV obtained from electron emission spectroscopy and listed in Bearden and Burr.[26] Further discussion of these matters is given in Sec. IV.

IV. DISCUSSION

It was originally hoped that very careful measurements on strain-free films of the silver halides at the lowest temperatures would allow separation of exciton from band-to-band absorption. The situation is complicated, however, primarily because of very small exciton binding energy, spin-orbit effects, and electron-phonon interaction. As shown in Fig. 2, for example, the AgCl direct exciton peak is really two peaks separated by about 0.14 or 0.15 eV. This is consistent with an estimated minimum splitting of 0.103 eV for a hole in the $j=\frac{3}{2}$, $j=\frac{1}{2}$ chlorine valence bands.[27] It is interesting that the ratio of the lower- to the higher-

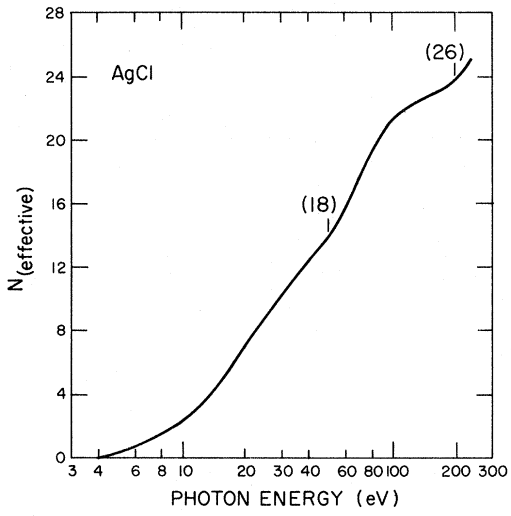

FIG. 10. Effective number of electrons contributing to optical absorption up to an energy E_0 plotted as the abscissa. Computed from Eq. (9) of the text.

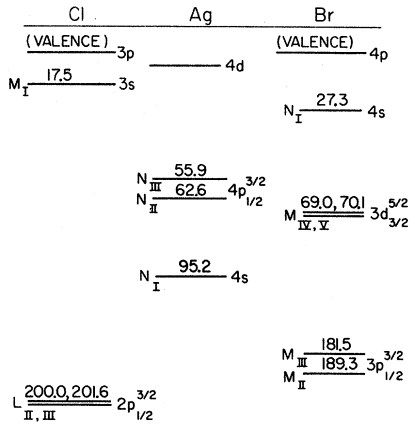

FIG. 11. Core and valence electron energy levels shown schematically for AgCl and AgBr from the tables of Bearden and Burr (Ref. 26).

energy peak is roughly 2 : 1, as expected from a simple theory and the $j = \frac{3}{2}, \frac{1}{2}$ state densities. In KCl the first peak is lower than the second and the ratio is considerably less than 1.[28] Onodera and Toyozawa[29] have shown how this behavior arises from electron-hole exchange interaction which, however, is appreciable only for small radius excitons. As indicated in Table II, indirect excitons in AgCl have small binding energies (0.023 eV) and large radii.[30,31] It is likely that direct excitons are similar in this respect, so that the exchange effects are small.

The spin-orbit doublet for AgBr is completely resolved, as can be seen in Figs. 3 and 5. Here, at low temperature, the first peak is at 4.276 eV and the second at 4.82 eV, so that the splitting is 0.54 eV, compared with an estimated minimum splitting for bromine of 0.432.[27] Again the ratio of the first to the second exciton strength is about 2 : 1. Most of the structure appearing in Fig. 5 was seen by Okamoto,[11] and is probably due to peaks in the joint state density at various regions throughout the Brillouin zone.

An interesting feature of the first exciton line in AgBr (shown in Fig. 3) is that the line is slightly asymmetrical with a just discernible shoulder on the high-energy side. This may be a result of the apparent linewidth, 0.08 eV, in part due to higher members of the exciton series and the band-to-band edge. On the other hand, the longitudinal optical phonon energy in AgBr is about 0.017 eV, so that one expects evidence for an exciton-phonon complex[18] on the high-energy side of the line. Above about 4.34 eV, it may be possible to approximately fit the band-to-band absorption by the Elliot theory.[32] Table II gives the observed exciton positions for both AgCl and AgBr along with the binding energies of Ascarelli[30] and the resulting direct energy gaps.

Next, we turn to an interpretation of the broad features of the extreme uv absorption of the silver halides above 30 eV. The various silver and halogen core levels (refer to Fig. 11) are indicated in Fig. 6, which best shows the absorption coefficients over a wide range. The first two broad peaks in the $N_{II,III}$ range are common to both AgCl and AgBr. The peak positions are approximately 49 and 61 eV for AgCl, and 48 and 59.5 eV for AgBr, giving respective separations of 12 and 11.5 eV. Similar structure has been seen by Haensel[23] in measurements on silver metal (shown by a dotted line in Fig. 6). The peaks in that work are at about 54 and 65 eV, giving a separation of 11 eV. The difference in peak positions between our work and that of Haensel may be due to a large, but not unusual, chemical shift between the metal and the silver halides. In addition, because of the strong underlying absorption apparent in Fig. 6 and also indicated by the low value of N_{eff} at 50 eV mentioned earlier, precise location of the peak positions is difficult. Nevertheless, it appears certain that these peaks are due to absorption by silver core states. The silver $4p$ levels lie at 55.9 and 62.6 eV,[26] giving a spin-orbit splitting of 6.7 eV. The calculated value of Herman and Skillman[33] is 4.9 eV. We believe that the separation of our peaks, 11–12 eV, is too large to be due to this spin-orbit splitting of the silver $4p$ states. The broadness of the second peak, and its position, at 61 eV for AgCl and 59.5 eV for AgBr, suggest that it is due to the unresolved spin-orbit doublet. The average of these peak positions, as given by Bearden, is 59.2 eV, which supports such an assignment. This leaves the peaks at 49 and 48 eV in AgCl and AgBr, respectively, unexplained on the basis of a simple one-electron absorption scheme. As we mentioned, there is strong underlying absorption in this region due to transitions from higher-lying states, principally the silver $4d^{10}$ electrons, and there may be interaction of these final state configurations with those resulting from the transitions from the silver $4p$ states. Obviously, further investigation is called for.

Referring once again to Fig. 6, additional struc-

TABLE II. Exciton binding energy and position of direct energy gap for AgCl and AgBr at liquid-helium temperature assuming direct and indirect binding energies are equal.

	Exciton peak position (eV)	Indirect exciton binding energy[a,b] (eV)	Direct energy gap (eV)
AgCl	5.13 ±0.05	0.023 ±0.002	5.15 ±0.05
AgBr	4.276 ±0.002	0.0164 ±0.0005	4.292 ±0.002

[a]Reference 10. [b]Reference 30.

ture for AgBr occurs in the small peaks at 72 and 75.5 eV. These are identified as absorption by bromine 3*d* levels. Here again, the peak separation is too large (3.5 eV) to be due to the spin-orbit splitting, given as 1.1 eV by Bearden and 1.2 eV by Herman and Skillman. The first peak, at 72 eV, is slightly broader than the one at 75.5 eV, and lies closer to the expected (69–70-eV) position of the 3*d* peaks. Thus the 72-eV peak may be the unresolved spin-orbit doublet. In this case, the peak at 75.5 eV would be due to transitions from the bromine 3*d* states to higher points in the conduction band. The remaining structure in AgBr is a step at 185 eV, identified as the transitions from bromine 3*p* states. The 3*p* edge of bromine should have a large spin-orbit splitting, 6.9 eV according to Herman and Skillman.[33] On the other hand, the measured absorption is very broad, and no identifiable structure is present beyond the absorption edge itself. This is probably due to matrix element and configuration interaction effects. Notice that the background absorption is nearly 2×10^5 cm^{-1}, whereas for the chloride in the same region the absorption is considerably less than 1×10^5 cm^{-1}.

The only structure appearing in the AgCl data at energies higher than the 61-eV peak discussed above is the $L_{II,III}$ or chlorine 2*p* absorption edge near 200 eV. This threshold, which is superimposed on a relatively low background, is shown in detail in Fig. 9. Various features of this spectrum, including the threshold at 197.6 eV, are listed in Table I. In general appearance the spectrum is somewhat similar to the chlorine $L_{II,III}$ structure of other alkali chlorides.[19,34–37] However, the peaks near threshold are less prominent for AgCl than for NaCl, RbCl, or KCl. At the same time, the uv exciton structure of AgCl is very sharp, as discussed above. The extreme uv structure of Fig. 9 did not change or sharpen very much upon cooling to low temperature. In our opinion, this is further evidence that exciton lines are relatively unimportant in this extreme part of the uv.[19,37] The detailed spectra near threshold can be understood largely in terms of the final band density of states when allowance is made for spin-orbit splitting of the initial core levels. Matrix elements certainly enter into the theoretical optical spectrum, but their effect is not dominant. This may be because the singularities observed in the alkali chloride arise from rather broad regions of *k* space away from the center of the zone, and considerable mixing of wave functions takes place.

The fact that the AgCl $L_{II,III}$ spectrum has an appearance like that of KCl[19] suggests that the conduction bands of these two materials are very similar. Figure 12 shows the band structure for AgCl in the ⟨100⟩ and ⟨111⟩ directions as calculated

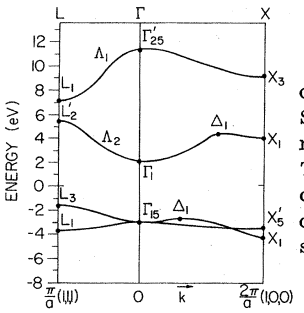

FIG. 12. Band structure of AgCl as calculated by Scop (Ref. 7) using the augmented-plane-wave method. The notation applies to the case where the origin of coordinates is located upon the silver ion.

by Scop[7] using the augmented-plane-wave method. The indirect band gap corresponds to transitions from L_3 to Γ_1[30] and the direct gap corresponds to transitions between Γ_{15} and Γ_1. A similar band diagram was given somewhat earlier by Bassani, Knox, and Fowler.[6] On the other hand, the published band structures for NaCl, KCl,[38] and RbCl[39] are quite different. In the alkali halides, the two bands which extend out in the ⟨100⟩ direction from the Γ_1 and $\Gamma_{25'}$ points cross, leading to an accidental degeneracy in this specific direction. Calculations have shown considerable state density concentrated near these crossing points, primarily away from the principal directions. This state density gives rise to prominent peaks observed for the alkali halides in the extreme uv.[19] It is not really clear if the band diagram for AgCl needs to be modified to include these crossing points. A carefully constructed theoretical optical spectrum might decide the issue, but this is a considerable task.

If we assume that Fig. 12 accurately represents the band structure of AgCl, the assignments given in the last column of Table I seem reasonable. The threshold at 197.6 eV corresponds to transitions from the Cl^- $L_{II,III}$ core level to Γ_1. The first rather weak peak 1 is due to a flat region of *k* space extending from Δ_1 to X_1, and this is accurately reproduced for the L_{II} core level at 2. In this way, the first structural features might be explained. Higher-lying band results and a theoretical spectrum are needed in order to unambiguously assign the higher peaks. It is interesting that the uv data of Figs. 4 and 7 show prominent absorption maxima in regions above threshold which correspond to peaks 1, 4, and 5 in Fig. 9. The uv and extreme uv spectra should be rather similar if a substantial part of the valence bands is relatively flat, as indicated in Fig. 12.

Atomic effects also enter into the soft x-ray spectra above threshold. For example, the structure just above threshold due to state density maxima will be superimposed upon a rising *p* to *d* background, as discussed by Fano and Cooper.[40] Such a background is quite apparent in Fig. 9, and we believe that this is the explanation for at least most

of the rise near 210 eV rather than double exciton processes.[34] For one thing, the direct band gap of AgCl is more nearly 5 eV rather than 9 eV, as in some alkali halides. This point is discussed in more detail elsewhere.[20] Multiple or collective excitations may also occur well above threshold. In view of the interesting results of Bauer and Spicer[9] in the uv, an attempt should be made to obtain detailed photoemission or luminescence information on the silver halides in the high-energy region.

ACKNOWLEDGMENTS

The authors wish to thank Dr. C. Gähwiller and Professor A. Barry Kunz for extensive help in connection with this work. We are also grateful to William C. Scheifley for his assistance in the extreme uv measurements. The help of the staff at the University of Wisconsin Physical Science Laboratory, especially E. M. Rowe, C. H. Pruett, and R. Otte, is greatly appreciated. The storage ring is supported by the U. S. Air Force of Scientific Research.

---

*Research supported by the U. S. Army Research Office (Durham) under Contract DA-31-124-ARO(D)-217 and the Advanced Research Projects Agency under Contract No. HC 15-67-C0221.

†Work performed in partial fulfillment of the requirements for the Ph. D. degree. Present address: Brookhaven National Laboratory, Upton, N. Y.

[1]F. Urbach, Phys. Rev. 92, 1324 (1953).

[2]F. Moser and F. Urbach, Phys. Rev. 102, 1519 (1956).

[3]F. C. Brown, T. Masumi, and H. H. Tippins, J. Phys. Chem. Solids 22, 101 (1961); F. C. Brown, J. Phys. Chem. 66, 2369 (1962).

[4]B. L. Joesten and F. C. Brown, Phys. Rev. 148, 919 (1966).

[5]F. Seitz, Rev. Mod. Phys. 23, 328 (1951).

[6]F. Bassani, R. S. Knox, and W. Beall Fowler, Phys. Rev. 137, A1217 (1965).

[7]P. M. Scop, Phys. Rev. 139, A934 (1965).

[8]A. D. Brothers and D. W. Lynch (private communication).

[9]R. S. Bauer and W. E. Spicer, Phys. Rev. Letters 25, 1283 (1970).

[10]G. Ascarelli, Phys. Rev. Letters 20, 44 (1968).

[11]Y. Okamoto, Nachr. Akad. Wiss. Goettingen, II. Math. Physik. Kl 14, 275 (1956).

[12]S. Tutihasi, Phys. Rev. 105, 882 (1957).

[13]J. J. White and J. W. Straley, J. Opt. Soc. Am. 58, 759 (1968).

[14]J. J. White III, Bull. Am. Phys. Soc. 13, 1720 (1968).

[15]M. Giammarinaro, M. B. Palma-Vittorelli, and M. U. Palma, Phys. Rev. Letters 21, 1382 (1968).

[16]F. Moser (private communication).

[17]C. Gähwiller, F. C. Brown, and H. Fujita, Rev. Sci. Instr. 41, 1275 (1970).

[18]R. Z. Bachrach and F. C. Brown, Phys. Rev. B 1, 818 (1970).

[19]F. C. Brown, C. Gähwiller, H. Fujita, A. B. Kunz, W. Scheifley, and N. Carrera, Phys. Rev. B 2, 2126 (1970).

[20]E. A. Stern, *Advances and Research*, Vol. 2 of *Solid State Physics*, edited by F. Seitz, E. A. Turnbull, and H. Ehrenreich (Academic, New York, 1968).

[21]H. R. Philipp and H. Ehrenreich, Phys. Rev. 129, 1550 (1963).

[22]L. W. Tilton, E. K. Plyler, and R. E. Stephens, J. Opt. Soc. Am. 40, 540 (1950); H. Schröter, Z. Physik 67, 24 (1931).

[23]R. Haensel, C. Kunz, T. Sasaki, and B. Sonntag, Appl. Opt. 7, 301 (1968).

[24]We are grateful to R. S. Bauer for furnishing White's data in tabular form. These values have been smoothed by Bauer from 3.3 to 4.3 eV to remove what is believed to be anomalous structure.

[25]C. J. Koester and M. P. Givens, Phys. Rev. 106, 241 (1957).

[26]J. A. Bearden and A. F. Burr, Rev. Mod. Phys. 39, 128 (1967).

[27]R. S. Knox and N. Inchauspé, Phys. Rev. 116, 1093 (1959).

[28]K. Teegarden and G. Baldini, Phys. Rev. 155, 896 (1967).

[29]Y. Onodera and Y. Toyozawa, J. Phys. Soc. Japan 22, 833 (1967).

[30]G. Ascarelli, Phys. Rev. 179, 797 (1969).

[31]F. C. Brown, Radiat. Effects 4, 223 (1970).

[32]R. J. Elliot, Phys. Rev. 108, 1384 (1957).

[33]F. Herman and S. Skillman, *Atomic Structure Calculations* (Prentice-Hall, Englewood Cliffs, N. J., 1963).

[34]T. Sagawa *et al.*, J. Phys. Soc. Japan 21, 2587 (1966).

[35]Y. Iguchi *et al.*, Solid State Commun. 6, 575 (1968).

[36]T. M. Zimkina and A. P. Lukirskii, Fiz. Tverd. Tela 7, 1455 (1965) [Sov. Phys. Solid State 7, 1170 (1965)].

[37]F. C. Brown, C. Gähwiller, A. B. Kunz, and N. O. Lipari, Phys. Rev. Letters 25, 927 (1970).

[38]A. B. Kunz, Phys. Rev. 175, 1147 (1968).

[39]A. B. Kunz, Phys. Status Solidi 29, 115 (1968).

[40]U. Fano and J. W. Cooper, Rev. Mod. Phys. 40, 441 (1968).